Water Research 265 (2024) 122267

Contents lists available at ScienceDirect

Water Research

journal homepage: www.elsevier.com/locate/watres

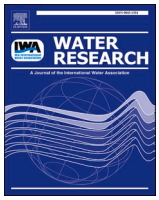

Persulfate activation by biochar and iron: Effect of chloride on formation of reactive species and transformation of *N,N*-diethyl-*m*-toluamide (DEET)

Yiling Zhuang [a,b], Stephanie Spahr [*,a,b], Holger V. Lutze [c,d,e], Christoph J. Reith [a,b], Nikolas Hagemann [f,g], Andrea Paul [h], Stefan B. Haderlein [b]

[a] Department of Ecohydrology and Biogeochemistry, Leibniz Institute of Freshwater Ecology and Inland Fisheries (IGB), Müggelseedamm 301, 12587 Berlin, Germany
[b] Department of Geosciences, Environmental Mineralogy and Chemistry, Eberhard Karls University of Tübingen, Schnarrenbergstr. 94-96, 72076 Tübingen, Germany
[c] Institute IWAR, Chair of Environmental Analytics and Pollutants, Technical University of Darmstadt, Franziska-Braun-Straße 7, 64287 Darmstadt, Germany
[d] IWW Water Centre, Moritzstraße 26, 45476 Mülheim an der Ruhr, Germany
[e] Centre for Water and Environmental Research (ZWU), University of Duisburg-Essen, Universitätsstraße 2, 45141 Essen, Germany
[f] Environmental Analytics, Agroscope, Reckenholzstrasse 191, 8046 Zürich, Switzerland
[g] Ithaka Institut gGmbH, Altmutterweg 21, 63773 Goldbach, Germany
[h] BAM Federal Institute of Materials Research and Testing, Richard-Willstaetter-Str. 11, 12489 Berlin, Germany

ARTICLE INFO

Keywords:
Water treatment
Oxidation processes
Organic contaminants
Fenton-like systems
Pyrogenic carbon
Probe compounds

ABSTRACT

Fenton-like processes using persulfate for oxidative water treatment and contaminant removal can be enhanced by the addition of redox-active biochar, which accelerates the reduction of Fe(III) to Fe(II) and increases the yield of reactive species that react with organic contaminants. However, available data on the formation of non-radical or radical species in the biochar/Fe(III)/persulfate system are inconsistent, which limits the evaluation of treatment efficiency and applicability in different water matrices. Based on competition kinetics calculations, we employed different scavengers and probe compounds to systematically evaluate the effect of chloride in presence of organic matter on the formation of major reactive species in the biochar/Fe(III)/persulfate system for the transformation of the model compound *N,N*-diethyl-*m*-toluamide (DEET) at pH 2.5. We show that the transformation of methyl phenyl sulfoxide (PMSO) to methyl phenyl sulfone ($PMSO_2$) cannot serve as a reliable indicator for Fe(IV), as previously suggested, because sulfate radicals also induce $PMSO_2$ formation. Although the formation of Fe(IV) cannot be completely excluded, sulfate radicals were identified as the major reactive species in the biochar/Fe(III)/persulfate system in pure water. In the presence of dissolved organic matter, low chloride concentrations (0.1 mM) shifted the major reactive species likely to hydroxyl radicals. Higher chloride concentrations (1 mM), as present in a mining-impacted acidic surface water, resulted in the formation of another reactive species, possibly $Cl_2^{\bullet-}$, and efficient DEET degradation. To tailor the application of this oxidation process, the water matrix must be considered as a decisive factor for reactive species formation and contaminant removal.

1. Introduction

Persulfate-based oxidation processes using peroxydisulfate (PDS) or peroxymonosulfate (PMS) have gained increasing interest for the removal of recalcitrant organic contaminants in water and wastewater treatment (Lee et al., 2020; Matzek and Carter, 2016; Zhou et al., 2019). Compared to hydroxyl radical ($^{\bullet}OH$)-based oxidation processes, which traditionally employ ozone, UV, or hydrogen peroxide (H_2O_2) (e.g. in the traditional Fenton process) (Miklos et al., 2018), persulfate-based oxidation processes have several advantages (Lee et al., 2020). For instance, persulfate salts enable cost-effective transportation and storage, and various methods allow the in situ production of highly reactive sulfate radicals ($SO_4^{\bullet-}$) by cleaving the peroxide bond in persulfate (Lee et al., 2020; Wacławek et al., 2017; Wang and Wang, 2018). One way to activate PDS is *via* reduced transition metals such as Fe(II) in a Fenton-like process at low pH (Nie et al., 2015; Wang et al., 2019a; Zhao et al., 2014). However, the rapid depletion of dissolved Fe(II) during PDS activation together with a low reduction rate of Fe(III) to Fe(II) and the accumulation of iron-containing sludge severely limit the applicability of this process (Luo et al., 2021a; Nie et al., 2015; Wang et al., 2019a; Zhao et al., 2014). To overcome these barriers, redox-active biochars have been successfully employed for catalytic

* Corresponding author.
E-mail address: stephanie.spahr@igb-berlin.de (S. Spahr).

https://doi.org/10.1016/j.watres.2024.122267
Received 9 February 2024; Received in revised form 23 July 2024; Accepted 12 August 2024
Available online 13 August 2024

activation of PDS in the presence of Fe(III) under acidic conditions (Liang et al., 2021; Lu et al., 2023; Tang et al., 2023; Wang et al., 2019b; Zeng et al., 2021). In this process, biochar has been shown to accelerate the reduction of Fe(III) to Fe(II), which activates PDS to reactive species for the transformation of organic contaminants, for instance in industrial wastewaters or other contaminated acidic waters (Liang et al., 2021; Lu et al., 2023; Tang et al., 2023; Wang et al., 2019b; Zeng et al., 2021).

However, there are contrasting findings on the major reactive species formed in the biochar/Fe(III)/PDS system (Liang et al., 2021; Tang et al., 2023; Wang et al., 2019b; Zeng et al., 2021). While some studies found evidence for radical-based processes, involving mainly $SO_4^{\bullet-}$ (Wang et al., 2019b; Zeng et al., 2021), others reported indications of non-radical processes, particularly involving Fe(IV) (Liang et al., 2021; Tang et al., 2023). Knowledge about the main reactive species is crucial already at an early stage of the development of a new oxidation process, such as the biochar/Fe(III)/PDS system, to identify suitable applications in terms of target contaminants as well as potential water matrix effects on treatment performance (Hübner et al., 2024). Identifying the major reactive species in oxidation processes is, however, challenging. Specialized instrumentation for the direct measurement of short-lived reactive species, e.g. by laser flash photolysis, is not readily available to most researchers (Burns et al., 2012; Nosaka and Nosaka, 2017; Zhou et al., 2017). Alternatively, probe compounds and scavengers play a crucial role as specific indicators for reactive species (Burns et al., 2012; Hübner et al., 2024; Nosaka and Nosaka, 2017; Rosario-Ortiz and Canonica, 2016), but must be selected and used with great care to avoid misinterpretation of the results. For instance, studies postulating the presence of Fe(IV) in the biochar/Fe(III)/PDS system are predominantly based on the observed transformation of methyl phenyl sulfoxide (PMSO) to methyl phenyl sulfone ($PMSO_2$) (Liang et al., 2021; Tang et al., 2023). There is, however, increasing concern about the use of PMSO as a specific probe compound for Fe(IV) (Chen et al., 2023; Lei et al., 2023; Yao et al., 2022), because the transformation of sulfoxide to sulfone is not specific to high-valent metal species (Chen et al., 2023) and there can be other pathways leading to $PMSO_2$ formation (Chen et al., 2023; Lei et al., 2023; Yao et al., 2022). In persulfate-based oxidation processes, it is unclear whether $SO_4^{\bullet-}$ can transform PMSO to $PMSO_2$.

Furthermore, little is known about the effects of water matrix components, in particular dissolved organic matter (DOM) and chloride (Cl^-), on the formation of reactive species in the heterogeneous biochar/Fe(III)/PDS system and how they affect contaminant transformation in real waters. In principle, $SO_4^{\bullet-}$ react more substrate-specific than $^{\bullet}OH$, leading to less kinetic inhibition by organic water matrix components (Hübner et al., 2024; Lee et al., 2020). However, Cl^- can shift $SO_4^{\bullet-}$-based processes to $^{\bullet}OH$ or reactive chlorine species, depending on the Cl^- concentration and the presence of DOM and bicarbonate (Bennedsen et al., 2012; Fang et al., 2012; Lutze et al., 2015a). Such effects of DOM and Cl^- on the formation of reactive species have previously been demonstrated in homogeneous PDS systems, in which PDS was activated by UV (Lutze et al., 2015a; Qian et al., 2016), heat (Bennedsen et al., 2012; Lutze et al., 2015b), or alkaline conditions (Bennedsen et al., 2012). In the heterogeneous biochar/Fe(III)/PDS system, systematic experimental evidence for the effects of Cl^- on the formation of reactive species and pollutant removal in presence of organic matter is still lacking.

The objectives of this study were therefore (i) to identify the major reactive species in the biochar/Fe(III)/PDS system and (ii) to investigate the effects of chloride in presence of organic matter on reactive species formation and organic contaminant removal. To this end, we established a biochar/Fe(III)/PDS system that degraded an organic model compound, the insect repellent *N,N*-diethyl-*m*-toluamide (DEET), at pH 2.5. DEET was selected because it cannot be effectively removed by conventional water treatment and is frequently detected in the aquatic environment (Costanzo et al., 2007; Stackelberg et al., 2007). In contrast to many model compounds usually studied in oxidation processes (e.g., sulfamethoxazole (Liang et al., 2021; Wang et al., 2019b)), the amide DEET is harder to oxidize (Lee et al., 2022; Padhye et al., 2014) and might serve as representative of other similar alkyl aromatic compounds (Dickenson et al., 2009). To determine the major reactive species formed in the biochar/Fe(III)/PDS system in the absence and presence of dissolved organic carbon (DOC) and Cl^-, we employed a combination of scavengers and probe compounds. Furthermore, we demonstrated the applicability of this heterogeneous oxidation process to a real water matrix.

2. Materials and methods

A list of all chemicals including supplier and purity is provided in Section S1 in the Supporting Information.

2.1. Biochar preparation and characterization

Biochar was produced in a PYREKA (Pyreg GmbH, Dörth, Germany) continuously operating screw reactor, which is described elsewhere (Hagemann et al., 2020). Beech wood was used as feedstock and pyrolyzed at 450 °C under N_2 atmosphere with a flow rate of 2 L min^{-1} and a residence time of 10 min. The biochar sample was ground to a particle size of < 200 μm using a ball mill (Figure S1) and stored in a desiccator until further use. For details on the biochar characterization, including electron exchange capacity, persistent free radicals, and elemental composition see Section S2.

2.2. DEET degradation with biochar, Fe(III), and PDS in pure water

Batch experiments were performed at room temperature in 40 mL amber glass vials on an overhead shaker. 30 mg of biochar was added to 30 mL deionized water to prepare a suspension of 1 g biochar L^{-1}. The initial pH of the suspension was adjusted to 2.5 with 0.25 M H_2SO_4. DEET was added to the suspension from an aqueous 10 mM stock solution to reach a nominal concentration of 50 μM. After 30 min contact time, sorption of DEET on the biochar reached an apparent equilibrium (Figure S2) and the measured aqueous DEET concentration was taken as initial value. Subsequently, 60 μL of Fe(III) was added from a freshly prepared 0.05 M aqueous Fe(III) sulfate stock solution to reach an initial concentration of 0.2 mM, followed by excess PDS addition (240 μL) from a 1 M aqueous stock solution to obtain an initial, nominal PDS concentration of 8 mM. At predefined time points, 1 mL sample was withdrawn and mixed with 100 μL of pure methanol (2 M in the sample, ≈ 9 % v/v) and 5.5 μL NaOH (10 mM in the sample, ≈ 1 % v/v, pH > 11) to quench the reaction and precipitate iron. Samples were filtered through 0.22 μm PES syringe filters (BGB Analytik, Germany; 88.5 ± 0.7 % DEET recovery) into 1.5 mL amber glass vials and stored in the dark at 4 °C until DEET analysis. The pH was measured at the beginning and the end of the experiment and remained constant at 2.5 ± 0.1, whereby no iron polymerization or precipitation was assumed to occur (Knight and Sylva, 1974). Control experiments were set up identically to assess the stability of DEET, sorption of DEET onto biochar, and reaction of DEET with (i) PDS, (ii) Fe(III), (iii) PDS and Fe(III), (iv) biochar and PDS, and (v) biochar and Fe(III). The experimental procedure is illustrated in Figure S3. To demonstrate the role of biochar for enhanced DEET transformation, we added three consecutive spikes of DEET (nominal concentration of 50 μM, each spike one hour apart) to the same 1 g biochar L^{-1} suspension containing 50 μM Fe(III) and 8 mM PDS. Samples were withdrawn at predefined time points for DEET analysis.

2.3. Effects of the water matrix on DEET transformation and reactive species

Surface water impacted by past lignite mining activities was sampled in the Greifenhainer Fließ, a tributary of the Spree River (51°45′28.8″N 14°08′54.0″E, Brandenburg, Germany) in December 2021. The water

sample was analyzed for pH, electrical conductivity, O_2 concentration, total and dissolved organic carbon, major ions such as Cl^- and SO_4^{2-}, as well as metals including iron species (see Section S18 and Table S3). DEET degradation experiments in acidic surface water followed the same procedure as described above, except that the pH of the 1 g biochar L^{-1} suspension was not adjusted, and no additional iron was added due to the low pH of 3.6 and high iron content (0.05 mM Fe(III)) of the surface water. Experiments in a synthetic water matrix (pH 3.6) containing 4.3 mg L^{-1} DOC (from Suwannee River humic acid) and 0.05 mM Fe(III) (from iron(III) sulfate) in the presence of 0.1 mM or 1 mM chloride also followed the procedure explained above.

2.4. Identification of reactive species using scavengers and probe compounds

Following the method suggested by Pestovsky and Bakac, 2006, 200 μM PMSO was added to a 1 g biochar L^{-1} suspension containing 0.2 mM Fe(III) and 8 mM PDS at pH 2.5. Batch experiments followed the procedure described above for DEET degradation. At predetermined time intervals, samples (1 mL) were withdrawn, quenched immediately with 100 μL of aqueous DMSO (2 M in samples, ≈ 9 % v/v), and analyzed for PMSO and $PMSO_2$. Control experiments were conducted with 200 μM PMSO and only PS, only biochar, only Fe(III), and combinations thereof. To investigate whether $PMSO_2$ is formed during the reaction of PMSO with $SO_4^{\bullet-}$, PDS was thermally activated at 60 °C in the presence of 200 μM PMSO and 20 mM *tert*-butanol (TBA), which was added to suppress formation of $^{\bullet}OH$ (93 % scavenged) from the reaction of $SO_4^{\bullet-}$ with small amounts of Cl^-(Lutze et al., 2015a). To study the reaction of PMSO with reactive chlorine species, PDS was thermally activated at 60 °C in the presence of 50 μM PMSO and 1 mM chloride. PMSO reacted with 95 % of the $SO_4^{\bullet-}$ to form reactive chlorine species. Experimental details and competition kinetics calculations are shown in Sections S12 and S13.

To investigate radical species in the biochar/Fe(III)/PDS system, we added different scavengers to a 1 g biochar L^{-1} suspension containing 50 μM DEET, 0.2 mM Fe(III), and 8 mM PDS. Methanol (300 mM final concentration) was added to completely scavenge > 99 % of both $SO_4^{\bullet-}$ (k ($SO_4^{\bullet-}$) = 1.1 × 10^7 M^{-1} s^{-1} (Neta et al., 1988)) and $^{\bullet}OH$ (k ($^{\bullet}OH$) = 9.7 × 10^8 M^{-1} s^{-1} (Buxton et al., 1988)). TBA (10 mM final concentration) was employed to scavenge 96 % of $^{\bullet}OH$ (k ($^{\bullet}OH$)= 6.0 × 10^8 M^{-1} s^{-1} (Buxton et al., 1988)) but only 14 % of $SO_4^{\bullet-}$ (k ($SO_4^{\bullet-}$) = 8.0 × 10^5 M^{-1} s^{-1} (Neta et al., 1988)). Additionally, DEET degradation experiments were conducted in the presence of different TBA concentrations (10 – 1000 mM), all resulting in > 95 % scavenging of $^{\bullet}OH$ and 14 % - 94 % scavenging of $SO_4^{\bullet-}$. Calculations of the fractions that react with an oxidant are based on the principles of competition kinetics (Dodd et al., 2006) and are described in Section S13. For competition kinetics experiments, 4-nitrobenzoic acid (*p*NBA) and 4-chlorobenzoic acid (*p*CBA) were added as probe compounds to a 1 g biochar L^{-1} suspension containing 0.2 mM Fe(III) and 8 mM PDS. Both *p*CBA and *p*NBA favor the reaction with radicals rather than Fe(IV) (Yang et al., 2023). *p*NBA readily reacts with $^{\bullet}OH$ (2.6 × 10^9 M^{-1} s^{-1} (Buxton et al., 1988)) but has a low reactivity towards $SO_4^{\bullet-}$ (≤ 10^6 M^{-1} s^{-1} (Neta et al., 1977)). *p*CBA reacts moderately with both $SO_4^{\bullet-}$ (3.6 × 10^8 M^{-1} s^{-1} (Neta et al., 1977)) and $^{\bullet}OH$ (5 × 10^9 M^{-1} s^{-1} (Buxton et al., 1988)). The competition kinetics approach can indicate the major reactive species present. For instance, hardly any degradation of *p*NBA together with the degradation of a high fraction of *p*CBA would be indicative of a $SO_4^{\bullet-}$-based process (Lutze et al., 2015a). The ratio of the first order degradation kinetics was obtained as the slope in a plot of ln(c/c_0) (*p*CBA) vs. ln(c/c_0) (*p*NBA) (Dodd et al., 2006; Lutze et al., 2015a). A $SO_4^{\bullet-}$-based oxidation process is characterized by a very small slope, while an $^{\bullet}OH$-based oxidation process leads to a theoretical slope of k ($^{\bullet}OH$ + *p*NBA)/k ($^{\bullet}OH$ + *p*CBA) of 0.52 (Buxton et al., 1988) (for further details on this methodology see Lutze et al., 2015a). Both probe compounds were added in low concentrations (4 μM for experiments in pure water and 5 μM for experiments in real water matrix) to ensure <10 % scavenging of $^{\bullet}OH$ and $SO_4^{\bullet-}$ by the probe compounds. A sorption control containing only *p*CBA, *p*NBA, and biochar was conducted to correct the transformation rates of *p*CBA and *p*NBA for sorption (Section S14, Figure S15). A control containing only *p*CBA, *p*NBA, and PDS showed no transformation of the probe compounds in the reaction time (Figure S16).

2.5. Analytical methods

The concentrations of DEET, PMSO, $PMSO_2$, *p*CBA, and *p*NBA were quantified by HPLC (1200 Series, Agilent) with UV–vis detection at 210 nm for DEET, 230 nm for PMSO, 215 nm for $PMSO_2$, 234 nm for *p*CBA, and 262 nm for *p*NBA. Aqueous samples were analyzed using an Agilent ZORBAX Eclipse XDB-C18 column (4.6 mm x 150 mm, 5 μm) and a ZORBAX Eclipse XDB-C18 guard cartridge. For DEET analysis, 10 μL of sample was injected and the eluent mixture consisted of 60 % methanol and 40 % water (pH 3, 1 mM H_2SO_4) at a flow rate of 0.5 mL min^{-1}. Concentrations were quantified by external calibration from 2 to 100 μM. For PMSO and $PMSO_2$ analysis, 20 μL of sample was injected and the mobile phase consisted of 75 % water with 1 % formic acid and 25 % acetonitrile with a flow rate of 0.5 mL min^{-1}. PMSO and $PMSO_2$ concentrations were quantified by external calibration from 1 to 250 μM and 0.5 to 125 μM, respectively. Analysis of *p*CBA and *p*NBA was carried out by injecting 50 μL of sample with an eluent mixture of 70 % methanol and 30 % water (pH 3, 1 mM H_2SO_4) at a flow rate of 0.5 mL min^{-1}. Concentrations were quantified by external calibration from 0.025 to 5 μM.

The fraction of a reactive species, f, reacting with a certain compound in competition with other substrates can be calculated with the corresponding known concentrations and reaction rate constants (Lutze et al., 2015a, 2015b). The fraction corresponds to the concentration ($c_{compound}$) times the reaction rate constant ($k_{compound}$) of the compound at study, divided by the sum of the concentrations (c_1, c_2 to c_n) times the reaction rate constants (k_1, k_2 *to* k_n) of all substrates that can react with the reactive species according to eq. (1):

$$f = \frac{c_{compound} \cdot k_{compound}}{c_{compound} \cdot k_{compound} + c_1 \cdot k_1 + c_2 \cdot k_2 + \cdots + c_n \cdot k_n} \quad (1)$$

3. Results and discussion

3.1. DEET degradation by PDS activation with biochar and Fe(III)

As shown in Fig. 1a, DEET was efficiently degraded in the presence of biochar, Fe(III), and PDS resulting in 88 ± 3 % DEET removal within two hours under the given experimental conditions. DEET degradation followed pseudo-first order kinetics with a k_{obs} of (2.9 ± 0.1) × 10^{-4} s^{-1} (Figure S4) and a half-life time of 39 ± 4 min. In control batches with PDS only, biochar only, Fe(III) only, and combinations thereof, DEET removal was much less efficient (<5.5 – 29 %, Fig. 1a). Our results agree with previous studies also reporting enhanced contaminant transformation in the presence of biochar, Fe(III), and PDS using sulfamethoxazole or bisphenol A as model compounds (Liang et al., 2021; Tang et al., 2023; Wang et al., 2019b; Zeng et al., 2021).The accelerated DEET degradation in the biochar/Fe(III)/PDS system indicates biochar-mediated Fe(III) reduction leading to continuous PDS activation upon reaction with Fe(II) as reported previously (Liang et al., 2021; Tang et al., 2023; Wang et al., 2019b; Zeng et al., 2021).

We compared the degradation of DEET in the heterogeneous biochar/Fe(III)/PDS system with DEET degradation in a homogeneous Fe (II)/PDS reference system, both containing 8 mM PDS but different concentrations of Fe(III) and Fe(II), respectively (Fig. 1b). In the Fe(II)/PDS system, DEET removal within two hours reaction time increased with increasing Fe(II) to PDS ratios from 1:160 to 1:16, corresponding to Fe(II) concentrations of 0.05 mM to 0.5 mM, respectively. To achieve 87 % DEET degradation in the homogeneous reference system, 0.5 mM Fe (II) had to be applied with 8 mM PDS (Fe(II) to PDS ratio of 1:16). In the

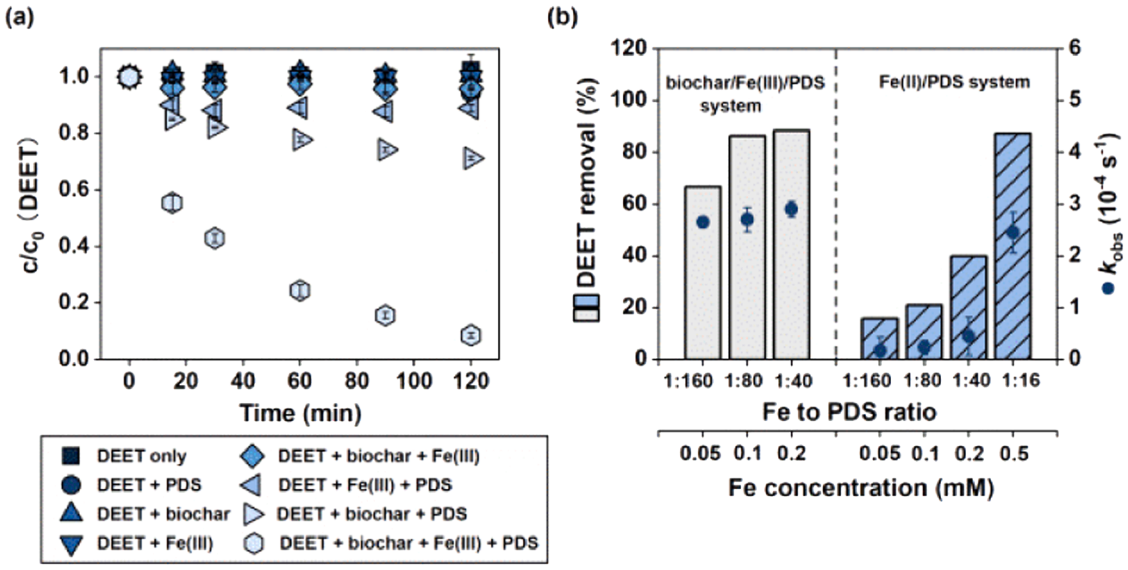

Fig. 1. (a) DEET transformation in the biochar/Fe(III)/PDS system and corresponding control experiments with DEET only, DEET and PDS, DEET and biochar, DEET and Fe(III), and combinations thereof. [Biochar] = 1 g L^{-1}, [Fe(III)] = 0.2 mM, [PDS] = 8 mM, $[DEET]_0 = c_0 \sim 40$ μM after sorption equilibrium, c = measured DEET concentration over time, pH 2.5. (b) DEET removal in the biochar/Fe(III)/PDS system (grey, solid bars) and the Fe(II)/PDS reference system (blue, patterned bars) at different molar Fe to PDS ratios and corresponding pseudo-first order rate constants (k_{obs}). [Fe(III)] = 0.05 - 0.2 mM for biochar/Fe(III)/PDS system, [Fe(II)] = 0.05 - 0.5 mM for Fe(II)/PDS system, [PDS] = 8 mM, $[DEET]_0 \sim 40$ μM, pH 2.5, reaction time = 2 h. Error bars indicate the standard deviation of triplicate experiments.

biochar/Fe(III)/PDS system, in contrast, 86 % DEET degradation was already obtained by adding 0.1 mM Fe(III), corresponding to an Fe(III) to PDS ratio of 1:80 (Fig. 1b). While dissolved Fe(II) can activate PDS in the homogeneous Fe(II)/PDS system, high input of Fe(II) is required due to rapid Fe(II) depletion and formation of Fe(III), which is only slowly reduced to Fe(II) by PDS (6.6×10^{-2} M^{-1} s^{-1}) (Hou et al., 2021; Luo et al., 2021a; Wang et al., 2019b).

Efficient DEET degradation in biochar suspensions with sub-stoichiometric Fe(III) to PDS addition indicates biochar-mediated enhanced Fe(III) reduction to Fe(II), which reacts with PDS. The Fe (III) formed can in turn be reduced back to Fe(II) by biochar. In fact, the biochar used here successfully reduced Fe(III) to Fe(II) (Figure S5) due to its redox-active properties. The biochar possessed a high electron donating capacity (EDC, 413 ± 22 μmol e^- (g biochar)$^{-1}$, Table S1), which is in the same order of magnitude as other biochars (Klüpfel et al., 2014). The biochar also contained a high concentration of persistent free radicals (PFR, $(3.50 \pm 0.40) \times 10^{19}$ spins (g biochar)$^{-1}$, Table S1), i.e. moieties with unpaired electrons that can contribute to the EDC (Luo et al., 2021b; Yuan et al., 2022) and were suggested to directly activate PDS (Fang et al., 2015; Kemmou et al., 2018; Luo et al., 2021b).

The addition of biochar to the Fe(II)/PDS system markedly increased the DEET degradation rate, indicating the role of biochar for Fe(III)/Fe (II) cycling (Figure S6). Further evidence for accelerated iron cycling was obtained from adding three consecutive spikes of DEET (50 μM each, 60 min apart) to the same 1 g L^{-1} biochar suspension containing 50 μM Fe(III) and 8 mM PDS (Figure S7). After three hours, 61 % of the added 150 μM DEET was removed, exceeding the present Fe(III) concentration by a factor of 1.8. In another experiment, the degraded DEET (739 μM) exceeded the Fe(III) present (200 μM) by a factor of 3.7 (Figure S8). The here used biochar thus enhanced Fe(III) reduction and facilitated PDS activation, as suggested by other studies (Liang et al., 2021; Tang et al., 2023; Wang et al., 2019b; Zeng et al., 2021), leading to the generation of reactive species and DEET degradation.

3.2. Identification of reactive species in the biochar/Fe(III)/PDS system

PMSO has been postulated as a specific probe compound to determine the presence of Fe(IV), as it reacts with the latter via a 2-electron transfer step to form a characteristic sulfone product, $PMSO_2$ (Pestovsky and Bakac, 2006). Fig. 2a shows PMSO transformation to $PMSO_2$ in the biochar/Fe(III)/PDS system. Within two hours, PMSO was completely oxidized following pseudo-first order kinetics with a reaction rate constant of $(3.2 \pm 0.2) \times 10^{-4}$ s^{-1} (Figure S9). The yield of $PMSO_2$ (i.e., mole of $PMSO_2$ formed per mole of PMSO transformed) was 62 %. Tang et al. (2023) and Liang et al. (2021) reported a similar conversion of PMSO to $PMSO_2$ (yields between 40 and 63 %) in the presence of low pyrolysis temperature biochars (< 500 °C), Fe(III), and PDS (Liang et al., 2021; Tang et al., 2023). Both studies concluded that Fe(IV) was present (Tang et al., 2023). However, there is increasing concern about the selectivity of PMSO as a specific probe compound for Fe(IV) (Chen et al., 2023; Lei et al., 2023; Yao et al., 2022). Lei et al. (2023) reported that PMS itself can transform PMSO to $PMSO_2$ (Lei et al., 2023). Chen et al. (2023) revealed that oxidation products of PMSO, formed via the reaction with $^{\bullet}OH$, can enhance $PMSO_2$ formation in the homogeneous Fenton reaction due to complexation of the PMSO oxidation products with Fe(III) (Chen et al., 2023).

Originally, PMSO was used to distinguish $^{\bullet}OH$ and Fe(IV) (Pang et al., 2011; Pestovsky and Bakac, 2006). The PMSO transformation products indicative for the presence of $^{\bullet}OH$ were defined as methanesulfinic acid and formaldehyde, whereas the reaction of PMSO with Fe(IV) formed $PMSO_2$ (Pang et al., 2011; Pestovsky and Bakac, 2006). Whether PMSO can be used in a similar way to distinguish between $SO_4^{\bullet-}$ and Fe(IV) has not been well investigated. In a clean $SO_4^{\bullet-}$-based reaction system, in which PDS was activated by heat and $^{\bullet}OH$ formation was suppressed by addition of TBA, PMSO was also transformed to $PMSO_2$ with 21 % yield (Figs. 2b and S10). No self-decomposition of PMSO was observed through heat (Figure S11) and PDS alone did not convert PMSO to $PMSO_2$ (Figure S12). Thus, in $SO_4^{\bullet-}$-based oxidation systems, PMSO cannot serve as a unique indicator for Fe(IV).

Yao et al. (2022) found similar results for thermal activation of PMS at 60 °C, which resulted in a $PMSO_2$ yield of 100 % (Yao et al., 2022). This much higher $PMSO_2$ yield might be due to the ability of PMS itself to transform sulfoxide to sulfone with considerable rate constants (Lei et al., 2023). Contrary results were reported by Wang et al. (2018), who found that $SO_4^{\bullet-}$ oxidized PMSO to biphenyl compounds rather than $PMSO_2$ during PDS activation by UV (Wang et al., 2018). However, the addition of HCl for pH adjustment likely shifted the reactive species formed from $SO_4^{\bullet-}$ to $^{\bullet}OH$ or reactive chlorine species (Ershov, 2004;

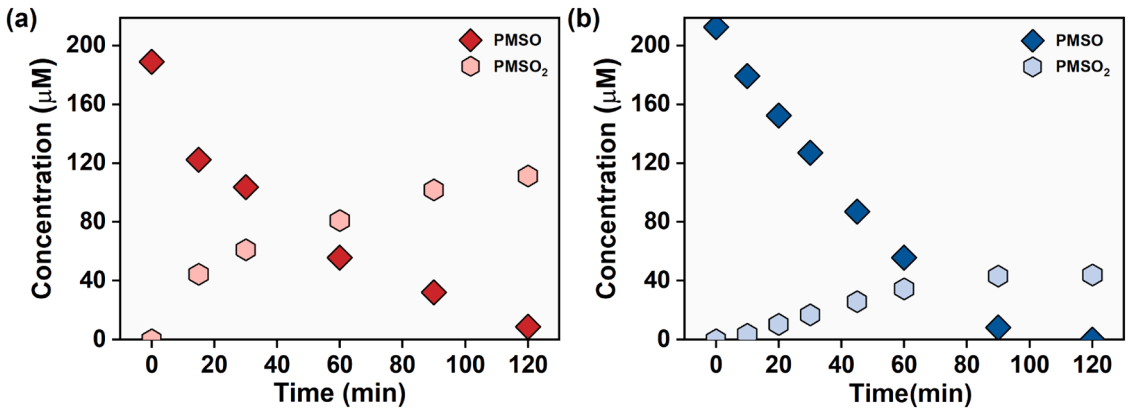

Fig. 2. (a) PMSO transformation and $PMSO_2$ formation in the biochar/Fe(III)/PDS system. [Fe(III)] = 0.2 mM, [Biochar] = 1 g L^{-1}, [PDS] = 8 mM, $[PMSO]_{0,\ after\ 30\ min\ sorption}$ = 189 μM, pH 2.5. (b) PMSO transformation and $PMSO_2$ formation in the heat/PDS control system. [PDS] = 8 mM, [PMSO] = 200 μM, [TBA] = 20 mM, pH 2.5, 60 °C in a water bath.

Lutze et al., 2015a; McElroy, 1990; U. Von Gunten, 2003) both of which do not transform PMSO into $PMSO_2$ as show in Figure S13 and other studies (Lai et al., 2022; Pang et al., 2011; Pestovsky and Bakac, 2006). Consequently, studies employing PMSO and $PMSO_2$ to distinguish Fe (IV) from $SO_4^{\bullet-}$ need to be carefully reassessed.

The higher $PMSO_2$ formation in the biochar/Fe(III)/PDS system (Fig. 2a) compared to the heat/PDS system (Fig. 2b) is likely due to the continuous reduction of Fe(III) to Fe(II), leading to PDS activation and formation of $SO_4^{\bullet-}$. Although we cannot strictly rule out the formation of Fe(IV), our results suggest that $SO_4^{\bullet-}$are the predominant reactive species in the biochar/Fe(III)/PDS system.

To further elucidate which reactive species were present in the biochar/Fe(III)/PDS system, we investigated DEET transformation in the presence of two scavengers, namely methanol and TBA. Note that competition kinetics calculations, as discussed in Section S13, are pivotal for a valid design and interpretation of scavenger experiments based on the fraction of reactive species scavenged. TBA, which solely scavenged $^{\bullet}OH$ at the applied dosages (96 % scavenging of $^{\bullet}OH$ and 14 % scavenging of $SO_4^{\bullet-}$), had no effect on DEET degradation. Methanol, which scavenged > 99 % of both $SO_4^{\bullet-}$ and $^{\bullet}OH$, completely stopped the reaction (Fig. 3a). These observations indicate that $SO_4^{\bullet-}$ are the dominant reactive species in the biochar/Fe(III)/PDS system. The involvement of $SO_4^{\bullet-}$was further verified by performing DEET degradation experiments in the presence of varying TBA concentrations from 10 mM to 1 M, resulting in an increased fraction of $SO_4^{\bullet-}$ scavenged from 14 % to 94 % (for detailed calculations see Section S13). With increasing TBA concentration, DEET degradation was increasingly inhibited (Figure S14), suggesting a $SO_4^{\bullet-}$-based oxidation process. In a purely $^{\bullet}OH$-based process, the scavenging effect would already be observed at TBA doses well below 10 mM.

To validate the formation of $SO_4^{\bullet-}$as major reactive species in the biochar/Fe(III)/PDS system, we employed *p*CBA and *p*NBA as probe compounds and conducted competition kinetics experiments. From the sorption-corrected competition kinetics plot in Fig. 3b and Figure S15, a nearly horizontal line was obtained, because hardly any *p*NBA was degraded, while *p*CBA was degraded to a large extent. These results clearly indicate that $SO_4^{\bullet-}$are the major reactive species in the biochar/Fe(III)/PDS system, in agreement with the scavenger experiments. The steady-state concentration of sulfate radicals $[SO_4^{\bullet-}]_{ss}$ was determined to be 2.69 × 10^{-11} M using *p*CBA as probe compound (Section S16 and Figure S17). It is noteworthy that *p*NBA and *p*CBA will hardly be reactive towards Fe(IV) (Yang et al., 2023).

Previous studies on the biochar/Fe(III)/PDS system collectively reported PDS activation by accelerated Fe(III) reduction to Fe(II) but did not provide a coherent picture concerning the reactive species involved (Liang et al., 2021; Tang et al., 2023; Wang et al., 2019b; Zeng et al., 2021). Liang et al., 2021 and Tang et al., 2023 reported an Fe(IV)-based non-radical pathway for the degradation of sulfamethoxazole and phenanthrene, respectively. Wang et al., 2019b and Zeng et al., 2021 proposed radical pathways, involving $SO_4^{\bullet-}$and $O_2^{\bullet-}$, respectively, for target compound transformation. This could be due to different biochars giving rise to different reactive species, or to inconclusive interpretation

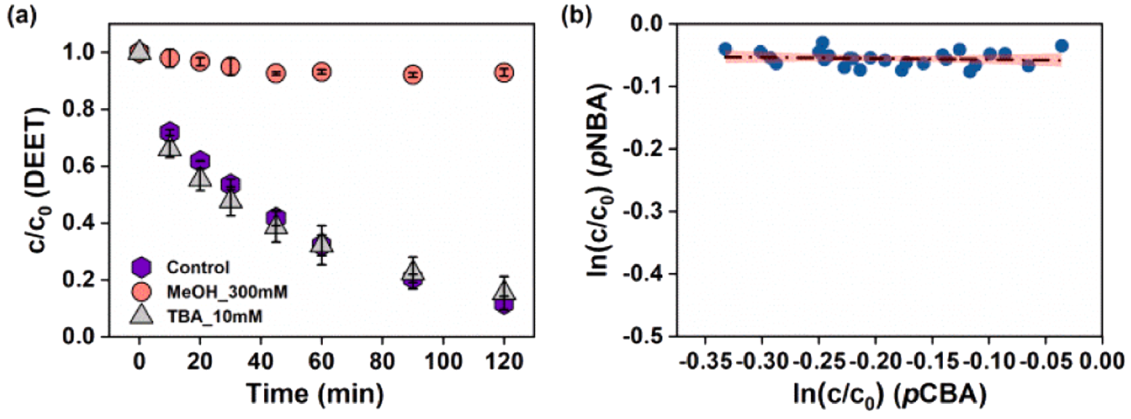

Fig. 3. (a) DEET degradation over time in the biochar/Fe(III)/PDS system in the absence (control) and presence of 300 mM methanol and 10 mM *tert*-butanol (TBA). [Biochar] = 1 g L^{-1}, [Fe(III)] = 0.2 mM, [PDS] = 8 mM, $[DEET]_0 = c_0 \sim 40$ μM, pH 2.5. (b) Sorption-corrected competition plot $\ln(c/c_0)$ of *p*CBA vs. *p*NBA in the biochar/Fe(III)/PDS system (slope −0.017 ± 0.031; intercept −0.058 ± 0.006). [Biochar] = 1 g L^{-1}, [Fe(III)] = 0.2 mM, [PDS] = 8 mM, $[pCBA]_{0,\ after\ 30\ min\ sorption}$ = 1.5 μM; $[pNBA]_{0,\ after\ 30\ min\ sorption}$ = 1.7 μM, pH 2.5. Red areas show the 95 % confidence intervals of the linear fit.

of results from scavenger or probe compound experiments. Scavengers and probe compounds used to diagnose reactive species should therefore be carefully chosen and caution should be advised if they do not react selectively or form secondary reactive species or unidentified products (Hübner et al., 2024; Willach et al., 2017). Indeed, superoxide and H_2O_2 may form in reactions of $SO_4^{\bullet-}$ with organic matter, but also in reactions of $^{\bullet}OH$ with scavengers such as TBA in the presence of oxygen (Flyunt et al., 2003; U. Von Gunten, 2003b). However, this would not affect the results of the present study, as superoxide and H_2O_2 seem to have no effect on the degradation of *p*NBA and *p*CBA, as their degradation perfectly matches the ratio of the reaction rate constants with $SO_4^{\bullet-}$ (Fig. 3b).

3.3. Effects of the water matrix on reactive species formation and DEET degradation

A biochar concentration of 1 g L^{-1} together with 8 mM PDS was applied to degrade 50 μM DEET in lignite mining-impacted surface water. This water was chosen due to its naturally low pH (3.6) and high iron concentration (0.05 mM, for more details see Supporting Information Section S17). DEET was almost completely degraded after two hours (Figure S18a). DEET disappearance in the acidic surface water followed pseudo-first order kinetics (Figure S18b) with a k_{obs} of (4.2 ± 0.1) × 10^{-4} s^{-1}. This value is approximately 1.5-times greater than the k_{obs} obtained for the transformation of DEET in ultrapure water at pH 2.5 (Fig. 1a and S4). The water matrix as well as the pH of the surface water thus did not inhibit DEET transformation, but rather enhanced the transformation of DEET, possibly due to the formation of reactive species other than sulfate radicals.

To investigate the major reactive species formed in this surface water matrix, *p*NBA and *p*CBA were employed in analogy to the competition degradation experiment shown in Fig. 3b. The competition plot of ln(c/c_0) (*p*CBA) vs. ln(c/c_0) (*p*NBA) shown in Fig. 4a yielded a slope of 0.8 ± 0.01. This slope is neither indicative for a $SO_4^{\bullet-}$-based process (leading to hardly any correlation), nor for an $^{\bullet}OH$-based process (leading to a slope of 0.52) (Lutze et al., 2015a). Water matrix constituents likely converted the $SO_4^{\bullet-}$-based process to an oxidation process governed by reactive species other than $SO_4^{\bullet-}$ or $^{\bullet}OH$. Table S3 shows that the mining-impacted surface water contained approximately 1 mM of Cl^- (31 mg L^{-1}). Cl^- reacts rapidly with $SO_4^{\bullet-}$ (k = 2.88 × 10^8 M^{-1} s^{-1}) to form chlorine atoms ($Cl^{\bullet}$), which can further react to other reactive species such as dichlorine radical anions ($Cl_2^{\bullet-}$) (Lutze et al., 2015a; McElroy, 1990).

To test the impact of Cl^- on the formation of reactive species in the biochar/Fe(III)/PDS system, we conducted competition kinetics experiments with *p*NBA and *p*CBA in a synthetic water matrix simulating the surface water characteristics (pH 3.6, 0.05 mM Fe(III), 4.3 mg L^{-1} DOC as Suwannee River humic acid) in the presence of 1 mM Cl^-. The competition plot in the synthetic water matrix (Fig. 4b) showed the same slope as obtained from the real mining-impacted surface water (Fig. 4a). This observation suggests that Cl^- caused the shift from $SO_4^{\bullet-}$ to potentially chlorine radical species.

Cl^-can react with $SO_4^{\bullet-}$ to form $Cl^{\bullet}$ (reaction (1) in Table 1), which in turn can react with H_2O to form $HOCl^{\bullet-}$ and eventually $^{\bullet}OH$ (see Lutze et al., 2015a and Section S21 for all reactions involved in the oxidation of Cl^-). In fact, an additional experiment with *p*NBA and *p*CBA in the same synthetic water matrix but low Cl^-concentration of 0.1 mM suggested an $^{\bullet}OH$-based oxidation process (Figure S19). At a low Cl^-concentration of 0.1 mM, the contribution of Cl^- to the overall $SO_4^{\bullet-}$scavenging was calculated to be 44 %, and the remaining 56 % is contributed by DOC (Section S20).

At a higher Cl^- concentration of 1 mM and low pH as present in the surface water, a significant amount of $Cl^{\bullet}$ may react with Cl^- to form

Table 1
Reactions involved in the oxidation of Cl^- with corresponding second order reaction rate constants and references.

No.	Reaction	Reaction rate constant	Unit	Ref.
(1)	$SO_4^{\bullet-} + Cl^- \rightarrow Cl^{\bullet} + SO_4^-$	2.7 × 10^8	M^{-1} s^{-1}	(McElroy, 1990)
(2)	$^{\bullet}OH + Cl^- \rightarrow HOCl^{\bullet-}$	4.3 × 10^9	M^{-1} s^{-1}	(Jayson et al., 1973)
(3)	$HOCl^{\bullet-} \rightarrow {}^{\bullet}OH + Cl^-$	6.1 × 10^9	s^{-1}	(Jayson et al., 1973)
(4)	$HOCl^{\bullet-} + H^+ \rightarrow Cl^{\bullet} + H_2O$	2.1 × 10^{10}	M^{-1} s^{-1}	(Jayson et al., 1973)
(5)	$Cl^{\bullet} + Cl^- \rightarrow Cl_2^{\bullet-}$	8 × 10^9	M^{-1} s^{-1}	(Nagarajan and Fessenden, 1985)

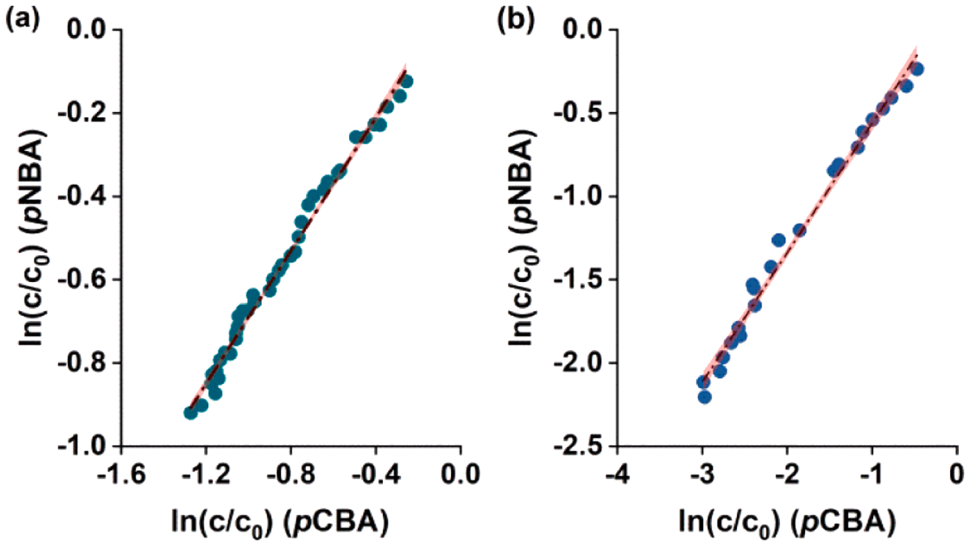

Fig. 4. (a) Sorption-corrected competition plot ln(c/c_0) of *p*CBA vs. *p*NBA in mining-impacted surface water (pH 3.6) containing 0.05 mM Fe(III), 1 mM Cl^-, and other constituents (Table S3) (slope 0.8 ± 0.01; intercept 0.11 ± 0.01). [Biochar] = 1 g L^{-1}, [PDS] = 8 mM, $[pCBA]_{0,\ after\ 30\ min\ sorption}$ = 1.64 μM; $[pNBA]_{0,\ after\ 30\ min\ sorption}$ = 2.31 μM. The reaction was initiated by adding PDS after 30 min sorption. (b) Sorption-corrected competition plot ln(c/c_0) of *p*CBA vs. *p*NBA in synthetic water containing 4.3 mg L^{-1} DOC (Suwannee River humic acid) and 1 mM Cl^- (slope 0.8 ± 0.02; intercept 0.2 ± 0.03). [Biochar] = 1 g L^{-1}, Fe(III) = 0.05 mM, [PDS] = 8 mM, $[pCBA]_{0,\ after\ 30\ min\ sorption}$ = 1.97 μM; $[pNBA]_{0,\ after\ 30\ min\ sorption}$ = 2.55 μM, pH 3.6 (adjusted with H_2SO_4). Red areas show the 95 % confidence intervals of the linear fit.

$Cl_2^{\bullet-}$ according to reaction (5) in Table 1. The scavenging of $SO_4^{\bullet-}$ and $^{\bullet}OH$ was mainly driven by Cl^- (≈ 90 %, reactions (1) – (4) in Table 1, for calculations see Section S20) to form $Cl^{\bullet}$. With excess Cl^-, the scavenging of $Cl^{\bullet}$ by Cl^- competes with the reaction forming $^{\bullet}OH$ (see Lutze et al., 2015a), resulting in the formation of $Cl_2^{\bullet-}$ (reaction (5)). At low pH values (< 4), the formation of $Cl_2^{\bullet-}$ is favored compared to neutral conditions (Ershov, 2004; Lutze et al., 2015a; U. Von Gunten, 2003). The rate constant of $Cl_2^{\bullet-}$ formation (reaction (5)) depends on both the concentration of Cl^- and H^+ and can be calculated using the rate constants of reactions (2) and (4) (Jayson et al., 1973), which can predict the major reactive species of radical-based oxidation processes at different conditions. While it was beyond the scope of this study to identify the reactive chlorine species, also Fang et al. (2012) suggested $Cl_2^{\bullet-}$ as predominant reactive species in a PDS-based oxidation process in the presence of high Cl^-concentrations (up to 100 mM) (Fang et al., 2012). In our study, DEET was removed efficiently in the presence of high Cl^- concentrations, suggesting a fast reaction between DEET and $Cl_2^{\bullet-}$. Although $Cl_2^{\bullet-}$ is less reactive than $SO_4^{\bullet-}$, its reactivity towards amides, like DEET, is high with reaction rate constants of 10^8 M^{-1} s^{-1} (Lei et al., 2019).

4. Conclusions

Our study demonstrates that the biochar/Fe(III)/persulfate system offers advantages compared to the Fe(II)/persulfate system because of accelerated reduction of Fe(III) to Fe(II) and formation of reactive species that react with organic contaminants. The type of reactive species formed, however, strongly depends on the water matrix. Using different scavengers and probe compounds, this study highlights that water matrix components, particularly chloride in presence of organic matter, can shift the formation of reactive species in the biochar/Fe(III)/PDS system. While $SO_4^{\bullet-}$ were the major reactive species in ultra-pure water, low chloride concentrations (0.1 mM) resulted in a change in reactive species, probably forming $^{\bullet}OH$. High chloride concentrations (1 mM) formed reactive chlorine species, likely $Cl_2^{\bullet-}$. Irrespective of the water matrix and chloride concentration, the organic model compound DEET was transformed upon application of the biochar/Fe(III)/PDS system at low pH. Our study demonstrates the effectiveness of the biochar/Fe(III)/PDS system using one model compound, but also provides the basis for further applications in water treatment because many other organic contaminants, especially those with similar or higher reactivity also react with the identified reactive species. For future applications, however, it must be noted that the biochar/Fe(III)/persulfate system, like the traditional Fenton process, requires a low pH value.

Knowledge about the effects of water matrix components on the formation of reactive species is crucial to tailor the biochar/Fe(III)/PDS system to specific applications such as industrial wastewater treatment or in situ chemical oxidation. While a mining-impacted water was used for this study, our findings provide a mechanistic understanding of the effect of water matrix components on the formation of reactive species in the biochar/Fe(III)/PDS system, which is highly relevant for contaminant abatement in other water matrices. As the water matrix plays a decisive role for the application of any oxidation process, future studies on the effects of other ions such as carbonate or phosphate ions on reactive species formation and contaminant transformation are recommended. Moreover, oxidation processes should combine the evaluation of the degradation efficiency of target pollutants with studies of the major reactive species and the formation of oxidation by-products and transformation products such as chlorate, bromate, or halogenated compounds in the respective water matrix.

CRediT authorship contribution statement

Yiling Zhuang: Writing – original draft, Visualization, Validation, Methodology, Investigation, Formal analysis, Data curation, Conceptualization. **Stephanie Spahr:** Writing – review & editing, Writing – original draft, Supervision, Resources, Methodology, Data curation, Conceptualization. **Holger V. Lutze:** Writing – review & editing, Methodology, Conceptualization. **Christoph J. Reith:** Writing – review & editing, Methodology, Investigation. **Nikolas Hagemann:** Writing – review & editing, Resources, Methodology, Investigation. **Andrea Paul:** Writing – review & editing, Methodology, Investigation. **Stefan B. Haderlein:** Writing – review & editing, Supervision, Resources, Methodology, Conceptualization.

Declaration of competing interest

The authors declare that they have no known competing financial interests or personal relationships that could have appeared to influence the work reported in this paper.

Data availability

Data will be made available on request.

Acknowledgments

This work was funded by the China Scholarship Council (CSC, File No 201904910454). We thank Claudia Schmalsch, Monika Hertel, Johanna Schlögl, and Guo-xiang Li for support in the laboratory, Tobias Goldhammer and Thomas Rossoll for providing and analyzing the surface water sample, and Viola Bartsch and Jannis Grafmüller of Ithaka for conductivity measurements.

Supplementary materials

Supplementary material associated with this article can be found, in the online version, at doi:10.1016/j.watres.2024.122267.

References

Bennedsen, L.R., Muff, J., Søgaard, E.G., 2012. Influence of chloride and carbonates on the reactivity of activated persulfate. Chemosphere 86, 1092–1097.
Burns, J.M., Cooper, W.J., Ferry, J.L., King, D.W., DiMento, B.P., McNeill, K., Miller, C.J., Miller, W.L., Peake, B.M., Rusak, S.A., 2012. Methods for reactive oxygen species (ROS) detection in aqueous environments. Aquat. Sci. 74, 683–734.
Buxton, G.V., Greenstock, C.L., Helman, W.P., Ross, A.B., 1988. Critical review of rate constants for reactions of hydrated electrons, hydrogen atoms and hydroxyl radicals ($^{\bullet}OH/^{\bullet}O^-$ in aqueous solution. J. Phys. Chem. Ref. Data 17, 513–886.
Chen, Y., Miller, C.J., Xie, J., Waite, T.D., 2023. Challenges relating to the quantification of ferryl (IV) Ion and hydroxyl radical generation rates using methyl phenyl sulfoxide (PMSO), phthalhydrazide, and benzoic acid as probe compounds in the homogeneous Fenton reaction. Environ. Sci. Technol. 57, 18617–18625.
Costanzo, S., Watkinson, A., Murby, E., Kolpin, D.W., Sandstrom, M.W., 2007. Is there a risk associated with the insect repellent DEET (N, N-diethyl-m-toluamide) commonly found in aquatic environments? Sci. Total Environ. 384, 214–220.
Dickenson, E.R.V., Drewes, J.E., Sedlak, D.L., Wert, E.C., Snyder, S.A., 2009. Applying surrogates and indicators to assess removal efficiency of trace organic chemicals during chemical oxidation of wastewaters. Environ. Sci. Technol. 43, 6242–6247.
Dodd, M.C., Buffle, M.O., von Gunten, U., 2006. Oxidation of antibacterial molecules by aqueous ozone: moiety-specific reaction kinetics and application to ozone-based wastewater treatment. Environ. Sci. Technol. 40, 1969–1977.
Ershov, B.G., 2004. Kinetics, mechanism and intermediates of some radiation-induced reactions in aqueous solutions. Russ. Chem. Rev. 73, 101–113.
Fang, G., Liu, C., Gao, J., Dionysiou, D.D., Zhou, D., 2015. Manipulation of persistent free radicals in biochar to activate persulfate for contaminant degradation. Environ. Sci. Technol. 49, 5645–5653.
Fang, G.D., Dionysiou, D.D., Wang, Y., Al-Abed, S.R., Zhou, D.M., 2012. Sulfate radical-based degradation of polychlorinated biphenyls: effects of chloride ion and reaction kinetics. J. Hazard. Mater. 227–228, 394–401.
Flyunt, R., Leitzke, A., Mark, G., Mvula, E., Reisz, E., Schick, R., von Sonntag, C., 2003. Determination of •OH, O_2•-, and hydroperoxide yields in ozone reactions in aqueous solution. J. Phys. Chem. B 107 (30), 7242–7253.
Hagemann, N., Schmidt, H.P., Kägi, R., Böhler, M., Sigmund, G., Maccagnan, A., McArdell, C.S., Bucheli, T.D., 2020. Wood-based activated biochar to eliminate organic micropollutants from biologically treated wastewater. Sci. Total Environ. 730, 138417.
Hou, K., Pi, Z., Yao, F., Wu, B., He, L., Li, X., Wang, D., Dong, H., Yang, Q., 2021. A critical review on the mechanisms of persulfate activation by iron-based materials: clarifying some ambiguity and controversies. Chem. Eng. J. 407, 127078.

Hübner, U., Spahr, S., Lutze, H., Wieland, A., Rüting, S., Gernjak, W., Wenk, J., 2024. Advanced oxidation processes for water and wastewater treatment–Guidance for systematic future research. Heliyon 10, e30402.
Jayson, G., Parsons, B., Swallow, A.J., 1973. Some simple, highly reactive, inorganic chlorine derivatives in aqueous solution. Their formation using pulses of radiation and their role in the mechanism of the Fricke dosimeter. J. Chem. Soc. Faraday Trans. 1 Phys. Chem. Condens. Phases 69, 1597–1607.
Kemmou, L., Frontistis, Z., Vakros, J., Manariotis, I.D., Mantzavinos, D., 2018. Degradation of antibiotic sulfamethoxazole by biochar-activated persulfate: factors affecting the activation and degradation processes. Catal. Today 313, 128–133.
Klüpfel, L., Keiluweit, M., Kleber, M., Sander, M., 2014. Redox properties of plant biomass-derived black carbon (biochar). Environ. Sci. Technol. 48, 5601–5611.
Knight, R.J., Sylva, R.N., 1974. Precipitation in hydrolysed iron (III) solutions. J. Inorg. Nucl. Chem. 36 (3), 591–597.
Lai, X., Huang, N., Pillai, S.C., Sarmah, A.K., Li, Y., Wang, G., Wang, H., 2022. Formation and transformation of reactive species in the Fe^{2+}/peroxydisulfate/Cl^- system. J. Environ. Manage. 316, 115219.
Lee, J., Von Gunten, U., Kim, J.H., 2020. Persulfate-based advanced oxidation: critical assessment of opportunities and roadblocks. Environ. Sci. Technol. 54, 3064–3081.
Lee, W.J., Bao, Y., Liangdy, A., Hu, X., Lim, T.T., 2022. Insights into the synergistic role of catalytic ceramic membranes for ozone and peroxymonosulfate activation towards effective recalcitrant micropollutant degradation and mineralization. Chem. Eng. J. 430, 132921.
Lei, Y., Cheng, S., Luo, N., Yang, X., An, T., 2019. Rate constants and mechanisms of the reactions of Cl• and Cl2•–with trace organic contaminants. Environ. Sci. Technol. 53, 11170–11182.
Lei, Y., Yu, Y., Lei, X., Liang, X., Cheng, S., Ouyang, G., Yang, X., 2023. Assessing the use of probes and quenchers for understanding the reactive species in advanced oxidation processes. Environ. Sci. Technol. 57, 5433–5444.
Liang, J., Duan, X., Xu, X., Chen, K., Wu, F., Qiu, H., Liu, C., Wang, S., Cao, X., 2021. Biomass-derived pyrolytic carbons accelerated Fe(III)/Fe(II) redox cycle for persulfate activation: pyrolysis temperature-depended performance and mechanisms. Appl. Catal. B Environ. 297, 120446.
Lu, J., Lu, Q., Di, L., Zhou, Yi, Zhou, Yanbo, 2023. Iron-based biochar as efficient persulfate activation catalyst for emerging pollutants removal: a review. Chin. Chem. Lett., 108357
Luo, H., Zeng, Y., He, D., Pan, X., 2021a. Application of iron-based materials in heterogeneous advanced oxidation processes for wastewater treatment: a review. Chem. Eng. J. 407, 127191.
Luo, K., Pang, Y., Wang, D., Li, X., Wang, L., Lei, M., Huang, Q., Yang, Q., 2021b. A critical review on the application of biochar in environmental pollution remediation: role of persistent free radicals (PFRs). J. Environ. Sci. 108, 201–216.
Lutze, H.V., Bircher, S., Rapp, I., Kerlin, N., Bakkour, R., Geisler, M., von Sonntag, C., Schmidt, T.C., 2015b. Degradation of chlorotriazine pesticides by sulfate radicals and the influence of organic matter. Environ. Sci. Technol. 49, 1673–1680.
Lutze, H.V., Kerlin, N., Schmidt, T.C., 2015a. Sulfate radical-based water treatment in presence of chloride: formation of chlorate, inter-conversion of sulfate radicals into hydroxyl radicals and influence of bicarbonate. Water Res 72, 349–360.
Matzek, L.W., Carter, K.E., 2016. Activated persulfate for organic chemical degradation: a review. Chemosphere 151, 178–188.
McElroy, W.J., 1990. A laser photolysis study of the reaction of SO_4^- with Cl^- and the subsequent decay of Cl_2^- in aqueous solution. J. Phys. Chem. 94, 2435–2441.
Miklos, D.B., Remy, C., Jekel, M., Linden, K.G., Drewes, J.E., Hübner, U., 2018. Evaluation of advanced oxidation processes for water and wastewater treatment – A critical review. Water Res 139, 118–131.
Nagarajan, V., Fessenden, R.W., 1985. Flash photolysis of transient radicals. 1. X_2^- with X= Cl, Br, I, and CN. J. Phys. Chem. 89, 2330–2335.
Neta, P., Huie, R.E., Ross, A.B., 1988. Rate constants for reactions of inorganic radicals in aqueous solution. J. Phys. Chem. Ref. Data 17, 1027–1284.
Neta, P., Madhavan, V., Zemel, H., Fessenden, R.W., 1977. Rate constants and mechanism of reaction of sulfate radical anion with aromatic compounds. J. Am. Chem. Soc. 99, 163–164.
Nie, M., Yan, C., Li, M., Wang, X., Bi, W., Dong, W., 2015. Degradation of chloramphenicol by persulfate activated by Fe^{2+} and zerovalent iron. Chem. Eng. J. 279, 507–515.
Nosaka, Y., Nosaka, A.Y., 2017. Generation and detection of reactive oxygen species in photocatalysis. Chem. Rev. 117, 11302–11336.
Padhye, L.P., Yao, H., Kung'u, F.T., Huang, C.H., 2014. Year-long evaluation on the occurrence and fate of pharmaceuticals, personal care products, and endocrine disrupting chemicals in an urban drinking water treatment plant. Water Res 51, 266–276.
Pang, S.Y., Jiang, J., Ma, J., 2011. Oxidation of sulfoxides and arsenic (III) in corrosion of nanoscale zero valent iron by oxygen: evidence against ferryl ions (Fe (IV)) as active intermediates in Fenton reaction. Environ. Sci. Technol. 45, 307–312.
Pestovsky, O., Bakac, A., 2006. Aqueous ferryl (IV) ion: kinetics of oxygen atom transfer to substrates and oxo exchange with solvent water. Inorg. Chem. 45, 814–820.
Qian, Y., Guo, X., Zhang, Y., Peng, Y., Sun, P., Huang, C.H., Niu, J., Zhou, X., Crittenden, J.C., 2016. Perfluorooctanoic acid degradation using UV–persulfate process: modeling of the degradation and chlorate formation. Environ. Sci. Technol. 50, 772–781.
Rosario-Ortiz, F.L., Canonica, S., 2016. Probe compounds to assess the photochemical activity of dissolved organic matter. Environ. Sci. Technol. 50, 12532–12547.
Stackelberg, P.E., Gibs, J., Furlong, E.T., Meyer, M.T., Zaugg, S.D., Lippincott, R.L., 2007. Efficiency of conventional drinking-water-treatment processes in removal of pharmaceuticals and other organic compounds. Sci. Total Environ. 377, 255–272.
Tang, Y., Dou, J., Lu, Z., Xu, J., He, Y., 2023. Accelerating Fe^{2+}/Fe^{3+} cycle via biochar to improve catalytic degradation efficiency of the Fe^{3+}/persulfate oxidation. Environ. Pollut. 316, 120669.
Von Gunten, U., 2003. Ozonation of drinking water: part II. Disinfection and by-product formation in presence of bromide, iodide or chlorine. Water Res 37, 1469–1487.
Von Gunten, U., 2003b. Ozonation of drinking water: part I. Oxidation kinetics and product formation. Water Res 37 (7), 1443–1467.
Wacławek, S., Lutze, H.V., Grübel, K., Padil, V.V., Černík, M., Dionysiou, D.D., 2017. Chemistry of persulfates in water and wastewater treatment: a review. Chem. Eng. J. 330, 44–62.
Wang, H., Guo, W., Yin, R., Du, J., Wu, Q., Luo, H., Liu, B., Sseguya, F., Ren, N., 2019b. Biochar-induced Fe(III) reduction for persulfate activation in sulfamethoxazole degradation: insight into the electron transfer, radical oxidation and degradation pathways. Chem. Eng. J. 362, 561–569.
Wang, J., Wang, S., 2018. Activation of persulfate (PS) and peroxymonosulfate (PMS) and application for the degradation of emerging contaminants. Chem. Eng. J. 334, 1502–1517.
Wang, S., Wu, J., Lu, X., Xu, W., Gong, Q., Ding, J., Dan, B., Xie, P., 2019a. Removal of acetaminophen in the Fe^{2+}/persulfate system: kinetic model and degradation pathways. Chem. Eng. J. 358, 1091–1100.
Wang, Z., Jiang, J., Pang, S., Zhou, Y., Guan, C., Gao, Y., Li, J., Yang, Y., Qiu, W., Jiang, C., 2018. Is sulfate radical really generated from peroxydisulfate activated by iron (II) for environmental decontamination? Environ. Sci. Technol. 52, 11276–11284.
Willach, S., Lutze, H.V., Eckey, K., Loeppenberg, K., Lüling, M., Terhalle, J., Wolbert, J. B., Jochmann, M.A., Karst, U., Schmidt, T.C., 2017. Degradation of sulfamethoxazole using ozone and chlorine dioxide-Compound-specific stable isotope analysis, transformation product analysis and mechanistic aspects. Water Res 122, 280–289.
Yang, B., Liu, H., Zhang, J., 2023. High-valent metals in advanced oxidation processes: a critical review of their identification methods, formation mechanisms, and reactivity performance. Chem. Eng. J. 460, 141796.
Yao, J., Wu, N., Tang, X., Wang, Z., Qu, R., Huo, Z., 2022. Methyl phenyl sulfoxide (PMSO) as a quenching agent for high-valent metal-oxo species in peroxymonosulfate based processes should be reconsidered. Chem. Eng. J. Adv. 12, 100378.
Yuan, J., Wen, Y., Dionysiou, D.D., Sharma, V.K., Ma, X., 2022. Biochar as a novel carbon-negative electron source and mediator: electron exchange capacity (EEC) and environmentally persistent free radicals (EPFRs): a review. Chem. Eng. J. 429, 132313.
Zeng, L., Chen, Q., Tan, Y., Lan, P., Zhou, D., Wu, M., Liang, N., Pan, B., Xing, B., 2021. Dual roles of biochar redox property in mediating 2, 4-dichlorophenol degradation in the presence of Fe^{3+} and persulfate. Chemosphere 279, 130456.
Zhao, L., Hou, H., Fujii, A., Hosomi, M., Li, F., 2014. Degradation of 1, 4-dioxane in water with heat-and Fe^{2+}-activated persulfate oxidation. Environ. Sci. Pollut. Res. 21, 7457–7465.
Zhou, L., Sleiman, M., Ferronato, C., Chovelon, J.M., Richard, C., 2017. Reactivity of sulfate radicals with natural organic matters. Environ. Chem. Lett. 15, 733–737.
Zhou, Z., Liu, X., Sun, K., Lin, C., Ma, J., He, M., Ouyang, W., 2019. Persulfate-based advanced oxidation processes (AOPs) for organic-contaminated soil remediation: a review. Chem. Eng. J. 372, 836–851.